Haltiwanger, R. C., Burns, J. M., Crockett, G. C., & Koch, T. H. (1978) *J. Am. Chem. Soc. 100*, 5110–5116.
Koetzle, T. F., Hamilton, W. C., & Parthasarathy, R. (1972) *Acta Crystallogr., Sect. B B28*, 2083–2089.
Lehmann, M. S., Koetzle, T. F., & Hamilton, W. C. (1972) *J. Cryst. Mol. Struct. 2*, 225–233.
Magnusson, S., Sottrup-Jensen, L., Peterson, T. E., Morris, H. R., & Dell, A. (1974) *FEBS Lett. 44*, 189–193.
Main, P., Hull, S. E., Lessinger, L., Germain, G., Declercq, J.-P., & Woolfson, M. M. (1978) *MULTAN: A System of Computer Programs for the Automatic Solution of Crystal Structures from X-ray Diffraction Data*, Universities of York, England, and Louvain, Belgium.
Märki, W., Oppliger, M., & Schwyzer, R. (1977) *Helv. Chim. Acta 60*, 807–815.
Motherwell, S., & Clegg, B. (1978) *PLUTO: Program for Plotting Molecular and Crystal Structures*, Cambridge Data Center, England.
Nelsestuen, G. L., Zythovicz, T. H., & Howard, J. B. (1974) *J. Biol. Chem. 249*, 6347–6350.
Parthasarathy, R. (1969) *Acta Crystallogr., Sect. B B25*, 509–518.
Rao, S. T. (1973) *Acta Crystallogr., Sect. B B29*, 1718–1720.
Satyshur, K. A., & Rao, S. T. (1979) *Acta Crystallogr., Sect. B B35*, 2260–2263.
Speakman, J. G. (1972) *Struct. Bonding (Berlin) 12*, 141–200.
Sperling, R., Furie, B. C., Blumenstein, M., Keyt, B., & Furie, B. (1978) *J. Biol. Chem. 253*, 3898–3906.
Spokane, R. B., Brill, R. V., & Gill, S. J. (1980) *Anal. Biochem. 109*, 137–145.
Stenflo, J., Fernlund, P., Egan, W., & Roepstorff, P. 1974) *Proc. Natl. Acad. Sci. U.S.A. 71*, 2730–2733.
Sutton, L. E., Ed. (1965) *Interatomic Distances and Configuration in Molecules and Ions*, The Chemical Society, London.
Willis, C. J. (1981) *J. Chem. Educ. 58*, 659–663.

Structure of Eukaryotic 5S Ribonucleic Acid: A Study of *Saccharomyces cerevisiae* 5S Ribonucleic Acid with Ribonucleases†

Roger A. Garrett* and Svend Ole Olesen

ABSTRACT: The structure of 5S RNA from *Saccharomyces cerevisiae* was examined by using ribonucleases A, S_1, T_1, and T_2 and a double helix specific cobra venom ribonuclease as probes. The 5′- and 3′-^{32}P-end labeled RNAs were examined, and this enabled a clear distinction to be made between primary and secondary cuts; a selection was also made for nicked, but intact, 5S RNA molecules. The relative degree of cutting was estimated, and the data were tested against secondary structural models. Support is provided for the minimal secondary structural model containing five helical regions; cobra venom ribonuclease cuts were detected in three of the five putative helical regions (helices I, II, and IV), and no single-strand-specific enzyme cuts were observed in the others (helices III and V). Of the putative non-double-helical regions, C_{10}–A_{11}, U_{33}, G_{37}–C_{39}, Ψ_{50}, G_{75}, and U_{90}–G_{91} were very accessible to the single-strand-specific ribonucleases; less accessible sites were G_{25}, G_{52}, U_{54}–A_{55}, C_{73}–C_{74}, and U_{83},G_{85}. Other putative non-double-helical regions A_{22}–A_{24}, C_{26}–C_{28}, C_{34}–C_{36}, C_{40}–C_{44}, U_{53}, A_{56}–G_{57}, A_{76}–A_{79}, and G_{101}–C_{105} were not cut by any ribonucleases and were assumed to be involved in the tertiary structure. Evidence implicating helices III and V in the RNA tertiary structure is also presented. An exceptional degree of flexibility in the sequence A_{22}–G_{57} was induced by primary cuts at U_{38} and C_{39}. The bulged nucleotides A_{63}/A_{64} in helix II and A_{84}/G_{85} in helix IV that have recently been proposed as protein recognition sites became selectively more accessible to the single-strand-specific ribonucleases as magnesium was removed from the RNA. Comparisons between the present results on a eukaryotic 5S RNA and those obtained earlier with *Escherichia coli* and *Bacillus stearothermophilus* 5S RNAs [Douthwaite, S., & Garrett, R. A. (1981) *Biochemistry 20*, 7301–7307] reveal a high level of structural homology and a few marked differences.

5S RNA is the smallest ribosomal RNA and is an integral part of the large ribosomal subunit; it has been localized, together with its bound proteins, in the neighborhood of the peptidyltransferase center in eubacterial ribosomes (Garrett et al., 1981). Although the RNA was thought to form an essential attachment site for elongator tRNAs, this has recently been refuted (Pace et al., 1982) and the precise role of the RNA remains unknown. Nevertheless, the relative structural simplicity of 5S RNA, and its native protein complexes, renders it an obvious choice for detailed studies on both ribosomal RNA secondary structure and the chemical specificity of protein–RNA interactions.

Phylogenetic sequence comparisons have proved to be a powerful aid in determining the secondary structures of both eubacterial (Fox & Woese, 1975) and eukaryotic 5S RNAs (Nishikawa & Takemura, 1974; Fox & Woese, 1975) and, more recently, of the large ribosomal RNAs (Noller & Woese, 1981). On the basis of such studies three double helices, I–III, which are also found in eubacterial 5S RNAs, were proposed at an early stage (Nishikawa & Takemura, 1974; Fox & Woese, 1975). More recently, there has been general agreement about two further helices, one that is analogous to helix IV in eubacterial 5S RNA and an additional one, V, that has no clear equivalent in eubacteria (Nishikawa & Takemura, 1974; Garrett et al., 1981; Luehrsen & Fox, 1981). Never-

† From the Division of Biostructural Chemistry, Kemisk Institut, Aarhus Universitet, DK-8000 Aarhus C, Denmark. *Received March 25, 1982.* The Danish Research Council provided a licentiate stipendium to S.O.O. and a temporary laboratory grant to R.A.G.

0006-2960/82/0421-4823$01.25/0

theless, several features of the secondary structure remain controversial. For example, an alternative cloverleaf model has been proposed (Luoma & Marshall, 1978), that retains helices I, III, and IV but rearranges helices II and V, which is compatible with much of the published structural data. Moreover, recent studies on archaebacteria 5S RNA structures have led Stahl et al. (1981) to propose that a series of non-Watson–Crick pairings occur in the vicinity of helices IV and V in all 5S RNAs.

In the present study, we have examined the structure of *Saccharomyces cerevisiae* 5S RNA by employing ribonucleases with different structural specificities; these include ribonucleases A, S_1, T_1, and T_2, which have a preference for single-stranded regions, and the *Naja naja oxiana* cobra venom ribonuclease, which is specific for double-helical structures (Vassilenko & Babkina, 1965).

In earlier studies of this type the cutting positions of single-strand-specific ribonucleases were generally assumed to occur in accessible non-base-paired regions [reviewed by Erdmann (1976)]. However, as was demonstrated recently, in a study on eubacterial 5S RNAs (Douthwaite & Garrett, 1981), this interpretation is subject to the strong reservation that a primary cut may produce a structural rearrangement that results in a secondary cut occurring at a position that is inaccessible in the native structure. Moreover, the secondary cut may then have more rapid kinetics than other primary cuts. As in the preceding work (Douthwaite & Garrett, 1981), we have tried to overcome this problem by performing mild digests and selecting, electrophoretically, for intact and minimally distorted RNA molecules containing a few nicks. The positions and intensities of the cuts were ascertained over a range of enzyme conditions by analyzing them on rapid sequencing gels using chemically sequenced 5S RNA samples as markers (Peattie, 1979). The use of both 3′- and 5′-end labeled RNA enabled us to distinguish between primary and secondary cuts.

This study was performed at 0 °C in the reconstitution buffer used for eubacterial ribosomes under conditions where protein–RNA complexes are stable, with a view, later, to compare the results from the complexes.

Materials and Methods

5S RNA from *S. cerevisiae* was isolated from 60S ribosomal subunits essentially by the method of Monier & Feunteun (1971). The procedure for 5′-end labeling was as follows. The RNA was dephosphorylated with calf intestine alkaline phosphatase (Boehringer-Mannheim) at 55 °C for 30 min and then purified on a 12% polyacrylamide slab gel (15 × 15 × 0.2 cm) containing 50 mM Tris–borate, pH 8.3, 1 mM EDTA, and 8 M urea at 30 V/cm for 1.5 h. RNA was extracted from the gel with 0.3 M ammonium acetate, pH 6.0, and 0.2% sodium dodecyl sulfate and precipitated twice with ethanol before reacting with [γ-^{32}P]ATP (Amersham) and T_4 polynucleotide kinase (P-L Biochemicals). The 3′-end labeling was attained with [^{32}P]pCp (Amersham) and RNA ligase (P-L Biochemicals) by using the procedure described by Peattie (1979).

The RNA was dissolved in TMK buffer (30 mM Tris-HCl, pH 7.8, 20 mM $MgCl_2$, and 300 mM KCl), renatured by heating at 65 °C for 5 min, and cooled slowly to room temperature before placing on ice. It was digested with ribonucleases A and S_1 (Sigma) and T_1 and T_2 (Sankyo) and *N. naja oxiana* cobra venom ribonuclease (gift of A. Butorin and S. Vassilenko) in the same TMK buffer at increasing ribonuclease: RNA ratios at 0 °C. The concentration ranges used were 1:3000 to 1:15 units/μg of RNA for RNase A, 2 to 100 units/μg of RNA for RNase S_1, 1:5000 to 1:500 units/μg of RNA for RNase T_1, 1:5000 to 1:50 units/μg of RNA for RNase T_2, and 1:300 to 1:100 units/μg of RNA for cobra venom RNase. Digestions with ribonuclease S_1 were performed in 100 mM sodium acetate, 10 mM $MgCl_2$, 1 mM $ZnCl_2$, and 100 mM KCl at pH 5. This buffer was added, after renaturation in TMK buffer, until the pH dropped to 5.0 in order to preserve, as effectively as possible, the native RNA conformation.

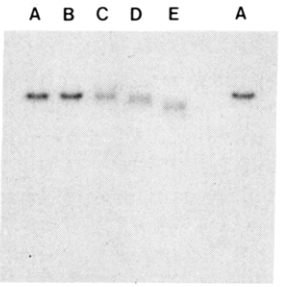

FIGURE 1: Digestion of 5S RNA with ribonuclease T_1. 5 μg of [^{32}P]pCp 3′-end labeled 5S RNA was treated with ribonuclease T_1 in 10 μL of TMK buffer for 30 min at 0 °C; (A) no ribonuclease; (B) 0.002 unit; (C) 0.004 unit; (D) 0.02 unit; (E) 0.04 unit. Samples were electrophoresed in a 12% polyacrylamide gel containing 40 mM Tris-HCl and 10 mM $MgCl_2$, pH 7.8, as described under Materials and Methods.

The digested samples were electrophoresed in 12% polyacrylamide gels (15 × 15 × 0.2 cm) containing 40 mM Tris-HCl and 10 mM $MgCl_2$, pH 7.8, 4 °C, at about 7 V/cm for 16 h with circulating buffer. The bands migrating alongside undigested 5S RNA were detected by autoradiography and excised; a few fragments that migrated faster than 5S RNA were also examined for their enzyme cuts. RNA was extracted from the gel in 0.3 M ammonium acetate and 0.2% sodium dodecyl sulfate, pH 5.5; for the ribonuclease T_2 treated sample an equal amount of phenol was used in the extraction to inactivate the comigrating ribonuclease. The RNA was precipitated twice with ethanol and dried.

Chemically sequenced 5S RNA samples were coelectrophoresed with ribonuclease-treated samples to facilitate identification of the cuts. The 3′-end labeled markers were made by chemical modification of heat-denatured RNA as described by Peattie (1979). Chemical sequencing of 5′-end labeled RNA yields partially heterogeneous fragments, and although the adenosine-specific reaction was used in some experiments, 5′-labeled markers were more often prepared by boiling the RNA sample for 15–45 min in loading buffer. Polyacrylamide gels (10%; 40 × 40 × 0.035 cm) were prepared as described earlier (Peattie, 1979); all samples were dissolved in loading buffer and coelectrophoresed at 50–60 W. The positions and intensities of ribonuclease or chemical cuts were deduced from autoradiograms.

Results

Isolation and Analysis of Digested 5S RNA. The 5S RNA was digested over a range of ribonuclease concentrations in order to produce a limited number of cuts in the molecule. Samples were coelectrophoresed with undigested 5S RNA. The result is shown in Figure 1 for a ribonuclease T_1 digest. The RNA bands in samples B and C, which comigrate with the undigested 5S RNA in sample A, were extracted from the gel. In some experiments, although not generally, the faster moving bands in tracks D and E were also analyzed. All samples were denatured by heating in 8 M urea and electrophoresed in RNA sequencing gels alongside 5S RNA samples that had been subjected either to the chemical sequencing

Table I: Primary Ribonuclease Cuts[a]

nucleotide	ribonuclease A	S_1	T_1	T_2	cobra venom
U_4					+
C_6					+++
G_7			(+)		+++
G_8					+
C_{10}	++			++	
A_{11}		+		++	
U_{12}		+			
A_{17}					+
C_{18}					+
C_{19}					++
A_{20}					+++
G_{21}					+
G_{25}			+		
U_{33}	++	+		+	
G_{37}			+++		
U_{38}		+++		++	
C_{39}	+++	+		+++	
Ψ_{50}		++			
A_{51}				(+)	
G_{52}			+		
U_{54}		+			(+)
A_{55}				+	
U_{59}					++
G_{60}					+
U_{62}					+
C_{73}				+	
C_{74}	(+)			+	
G_{75}			++		
G_{82}					++
U_{83}	+	(+)		+	
G_{85}			++		
U_{90}	+	+		+	
G_{91}		+	+++	+	
U_{96}					+
A_{97}					++
C_{98}					+
G_{99}					++
U_{114}					++
A_{117}					+

[a] The data are averaged from several experiments for each ribonuclease. The number of separate experiments performed, each involving digestion over a range of enzyme concentrations, is given for each ribonuclease with the number of experiments with 5′-end-labeled RNA preceding that for the 3′-end-labeled RNA: ribonuclease A (2, 3), S_1 (6, 6), T_1 (5, 3), and T_2 (5, 4) and cobra venom ribonuclease (5, 4). The quantitation system is as follows: +++ = strong cuts, ++ = intermediate cuts, and + = weak cuts; (+) indicates either very weak cuts or weak cuts that were not always detected. The cobra venom ribonuclease cuts at G_7 and U_6 were observed only on 5′- and 3′-end labeled samples, respectively. This does not fit our criterion of secondary cutting and both are included as primary cuts. The weak T_1 ribonuclease cut at G_7 is included although it was not seen on 5′-end labeled samples; it may have dissociated from the latter.

procedure of Peattie (1979) or to water hydrolysis. An autoradiogram showing the samples in Figure 1 digested with ribonuclease T_1 is depicted in Figure 2. All of the results for this ribonuclease, and for the others, are summarized in Tables I and II.

Distinguishing Primary and Secondary Cuts. A distinction was made between primary and secondary cuts by examining both 5′- and 3′-end labeled samples on sequencing gels. Primary cuts occur at accessible nucleotides in the native structure and are seen on both 5′- and 3′-end labeled samples and are listed in Table I. Secondary cuts occur as a result of, and subsequent to, a primary cut, and they are seen in either 5′- or 3′-end labeled samples but not in both; they occur at nucleotide bonds that are inaccessible to the particular ribonuclease in the native structure; they are listed in Table II.

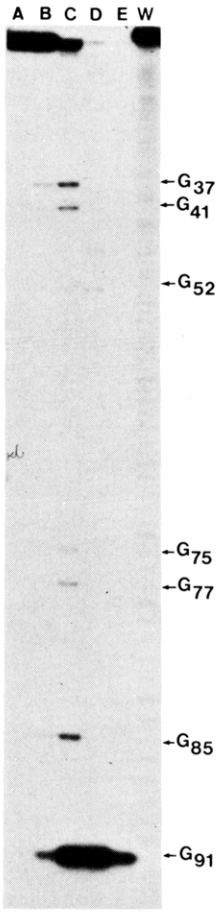

FIGURE 2: Sequencing gel with 5S RNA samples digested with ribonuclease T_1 in Figure 1. Samples were treated with increasing amounts of ribonuclease T_1 as described in the legend to Figure 1: (A) no ribonuclease; (B) 0.002 unit; (C) 0.004 unit; (D) 0.02 unit; (E) 0.04 unit. Samples were electrophoresed in the sequencing gel. W represents an RNA ladder formed by boiling in water for 30 min.

Table II: Secondary Cutting Positions[a]

nucleotide	ribonuclease A	S_1	T_1	T_2	end labeling	dependent on primary cut
U_{12}	+				3′	C_{10}
A_{22}–A_{24}		+		+	5′	U_{33}
C_{26}–U_{32}		+		+	5′	U_{33}
C_{34},C_{35}		(+)		+	5′	U_{38}
C_{36}	(+)			++	5′	U_{38}
G_{37}		++		+	5′	U_{38}
U_{38}	++				5′	C_{39}
C_{40}				++	3′	C_{39}
G_{41}			+	+	3′	G_{37}/C_{39}
A_{42}–C_{44}		+		+	3′	C_{39}
A_{51}		+			3′	Ψ_{50}
G_{52},U_{53}				+	3′	A_{51}
A_{55}		+			3′	U_{54}
A_{56}		+		(+)	3′	U_{54}/A_{55}
G_{57}				+	3′	A_{55}
G_{75}–A_{79}				+	3′	C_{74}
G_{77}			+		3′	G_{75}
G_{80},G_{82}			+		5′	G_{85}
A_{84}–U_{86}				+	3′	U_{83}
G_{88}				+	5′	G_{91}
G_{89}		(+)	+		5′	G_{91}
G_{91}–A_{92}				+	3′	U_{90}

[a] The same system of quantitation is used as that for Table I.

Secondary cutting was most prolific for ribonucleases S_1 and T_2. An example for the latter enzyme is shown in Figure 3 for both 5′- and 3′-end labeled RNA. The bands at U_{38} and C_{39} are visible on both 5′- (I) and 3′-end labeled samples (II)

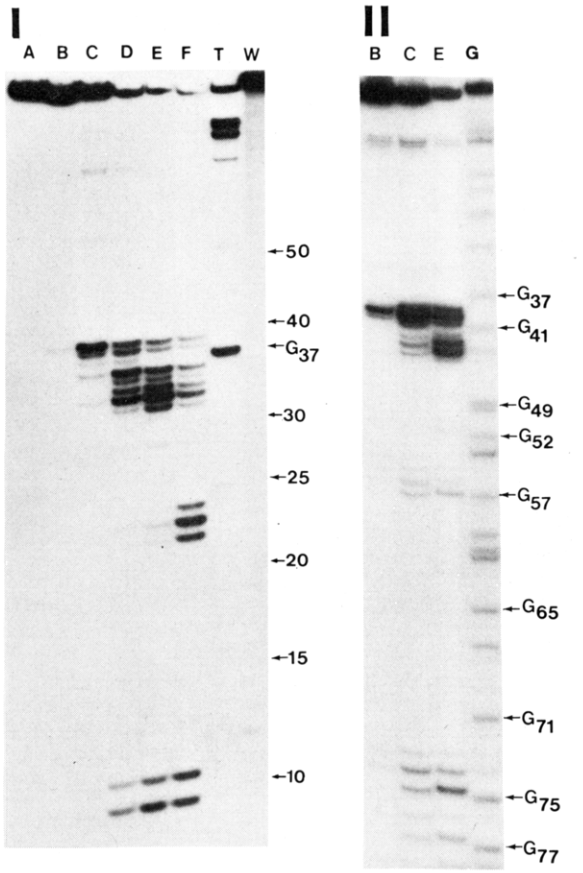

FIGURE 3: Digestion of 5S RNA with ribonuclease T_2: (I) 5′-end labeled and (II) 3′-end labeled RNA. 5 μg of RNA was digested in 10 μL of TMK buffer for 20 min at 0 °C with (A) no ribonuclease, (B) 0.005 unit, (C) 0.01 unit, (D) 0.05 unit, (E) 0.1 unit, and (F) 0.5 unit. The intact RNA band was purified by polyacrylamide gel electrophoresis prior to running on the sequencing gel. Ribonuclease T_1 (T) and water hydrolysis (W) tracks are shown for the 5′-labeled sample, and a guanosine (G) chemical sequencing track is given for the 3′-end labeled sample.

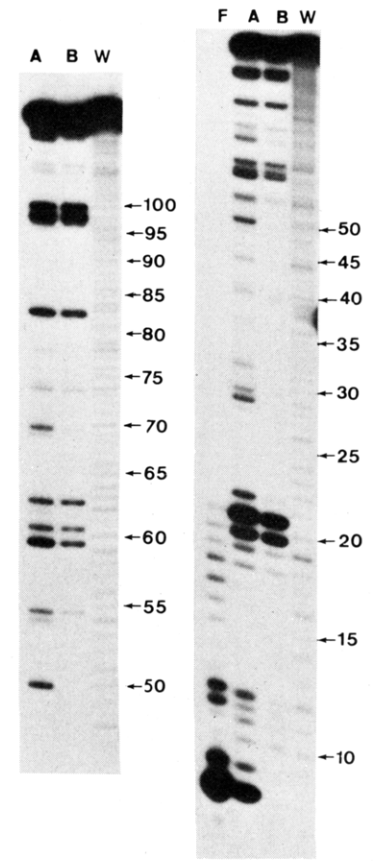

FIGURE 4: Sequencing gel of 5S RNA digested with cobra venom ribonuclease. 5 μg of RNA was digested with 0.05 unit of cobra venom ribonuclease for 30 min at 0 °C in 10 μL of TMK buffer and extracted with phenol: (A) sample applied directly after phenol extraction; (B) sample purified on a magnesium-containing polyacrylamide gel (see Materials and Methods). F corresponds to a fragment isolated from the gel used for purifying sample B. W represents the water hydrolysis ladder that was formed as described in Figure 2.

and are, therefore, primary cuts. Exclusive to the 5′-end labeled samples, however, are a series of strong cuts at nucleotides C_{34}, C_{35}, C_{36}, and G_{37}, which we infer are secondary to the primary cuts at U_{38} and C_{39}. Exclusive to the 3′-end labeled samples are strong cuts at C_{40}, G_{41}, A_{42}, and U_{43}, which we infer are also secondary to the primary cuts.

Quantitation of Cuts. A simple (+) system is used in Table I for the quantitation of primary cuts that is based on a comparison of several autoradiograms exhibiting a concentration range of a given ribonuclease. It is difficult to obtain a better quantitation partly because of the problem of dissociating primary and secondary effects. The intensities of the secondary cuts in Table II were estimated relative to the primary cuts, under conditions where approximately 20–50% of the 5S RNA molecules remain uncut.

Identification of Primary Cuts. (*a*) *Unstructured Regions.* Three regions are very accessible to the single-strand-specific ribonucleases at C_{10}–U_{12}, G_{37}–C_{39}, and U_{90},G_{91} and here the bases are probably unstacked. In addition, weaker breaks were observed at G_{25}, U_{33}, Ψ_{50}, G_{52}, U_{54}–A_{55}, C_{73}–G_{75}, and U_{83}–G_{85}, and these nucleotides are less accessible and weakly stacked or nonstacked. These data are summarized in Table I and Figure 5.

(*b*) *Double-Helical Regions.* These were probed with cobra venom ribonuclease, and the results are illustrated in Figure 4. Multiple cuts were found in the putative helices I, II, and IV drawn in Figure 5. Although no cuts were detected in helices III and V, no single-strand-specific cuts were observed there either. There is still no direct experimental evidence to support the latter helices, but it is possible that they are inaccessible within the tertiary structure. Digests are shown for the 5′-labeled sample in Figure 4. One sample (B) was, as usual, electrophoresed after digestion to select for intact but nicked molecules whereas the other sample (A) was loaded directly on the sequencing gel. Although the strongest bands are common to both samples, additional cobra venom ribo-

Table III: Additional Cobra Venom Ribonuclease Cuts Not Found in the Main Conformer Isolated on Magnesium-Containing Gels[a]

nucleotide	degree of cut	helix
C_{28}	+	III
C_{29}	+	
U_{31}	+	
C_{35}	(+)	
C_{36}	(+)	
C_{69}	+	V
G_{77}	(+)	
U_{106}	(+)	V
C_{107}	(+)	
A_{108}	(+)	
G_{115}	++	I

[a] The experiment was performed as described in the legend to Figure 4. After digestion no electrophoretic selection was made for the intact 5S RNA, as illustrated in Figure 1, prior to running the sequencing gel. The quantitation is the same system used as that in Tables I and II.

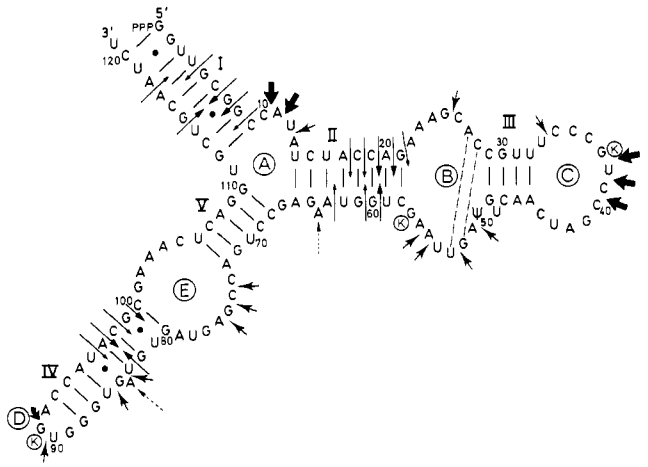

FIGURE 5: Secondary structural model for *S. cerevisiae* 5S RNA. The five helical regions are defined and numbered according to Garrett et al. (1981) and Luehrsen & Fox (1981); the loop region nomenclature of the latter study is used. Broken lines indicate possible additional paired bases, and these are considered further in the text. The putative bulged nucleotides in helices II and IV are indicated by striated arrows. The full arrows mark the primary cutting positions of nucleases A, S_1, T_1, and T_2, which all exhibit a strong single-strand preference: large arrows correspond to strong cuts and small arrows indicate weak cuts. Secondary cutting positions are not shown. If a nucleotide is cut strongly by one ribonuclease and weakly by another, the cut is represented with a large arrow. Arrows drawn into helices and across the polynucleotide chain represent the sites of the cobra venom ribonuclease cuts: again the arrow size defines the degree of cutting. Further details of the enzyme cuts are given in Tables I–IV. Strong kethoxal modification sites identified by Nishikawa & Takemura (1978) in *T. utilis* 5S RNA are indicated by K's.

nuclease cuts occur in the latter sample, which are listed in Table III with their relative intensities; they are considered further below. Five of the bands that appear only in sample A, at C_{10}, U_{12}, C_{39}, C_{44}, and U_{54}, are not cobra venom ribonuclease cuts since they are not displaced from the calibration ladder (see Figure 4); the former four cuts were present as weak bands in the undigested RNA sample. The absence of the strong cut at G_7 in sample B probably indicates a selective loss of this fragment during the ethanol precipitations after the gel purification step.

The fact that we only observed additional cobra venom ribonuclease cuts when we did not select for the native conformer suggests that the RNA was partially unfolded when the extra cuts were induced and, consequently, had an altered mobility in the magnesium gel. Another possible explanation is that we are detecting an alternative conformer with altered base pairing (as occurs, for example, with the A and B conformers of *Escherichia coli* 5S RNA); the latter is unlikely, though, because the main cuts are common to both samples in Figure 4.

Secondary Cuts. These generally appear adjacent to primary cuts and are listed in Table II. Most occurred with ribonucleases S_1 and T_2, which may reflect the sensitivity of these enzymes to local flexibilities in the RNA structure. The largest secondary effects, as indicated in Figure 3, result from the primary cuts at U_{38}/C_{39}. The polynucleotide chain tends to open toward both 5′ and 3′ ends of the molecule. Weaker cuts are also visible which intensify under stronger digestion conditions and extend right back to nucleotides A_{22} and G_{57}, respectively, indicating flexibility, or breathing, of the RNA as far back as helix II. Similarly, loops D and E and helix IV are progressively digested mainly as a result of primary cuts in these loops and in the putative bulge region of helix IV (see Figure 5). An RNA core constituting helices I, II, and V is highly resistant.

Table IV: Effect of Magnesium on Ribonuclease T_2 Digestion of 5S RNA[a]

nucleotide	degree of cutting: 20 mM Mg^{2+}	degree of cutting: 0 mM Mg^{2+}	helix
U_{62}	–	(+)	II
A_{63}	–	+	II
A_{64}	–	(+)	II
U_{83}	+	++	IV
A_{84}	–	++	IV
G_{85}	–	+	IV

[a] The experiment was performed by digesting 5 μg of 5S RNA with ribonuclease T_2 in the standard digestion buffer containing 20 mM magnesium. The samples were titrated with increasing amounts of 0.1 M Na_2EDTA prior to adding 10^{-3} unit of ribonuclease to each sample. The results show the intensities of the bands at a molar equivalence of $MgCl_2$ and Na_2EDTA.

Examination of both 3′- and 5′-end labeled samples revealed no evidence for secondary cutting with the cobra venom ribonuclease.

Effect of Magnesium on the RNA Structure. After the RNA was renatured in ribosomal reconstitution buffer, the magnesium ions were progressively depleted by adjusting aliquots of RNA to increasing EDTA concentrations. Digestion with ribonuclease T_2, under the lower ribonuclease conditions used in the above studies (10^{-3}–10^{-2}) unit/μg of RNA), demonstrated that the RNA was very resistant to the ribonuclease even in the absence of free Mg^{2+} ions. Two changes were observed, however. First, doubling of bands was detected that resulted from partial removal of the 3′-terminal Cp. This suggested that the 3′-terminal pCpU was stacked on helix I in the presence of Mg^{2+}. Second, the kinetics of cutting in the accessible regions, indicated in Table I, increased especially within the region A_{22}–G_{57} and C_{73},C_{74}. More dramatic, however, were the effects at the putative bulged nucleotides A_{63},A_{64} in helix II and A_{84},G_{85} in helix IV. Cuts were observed for the first time in the former and stronger cuts occurred in the latter. The results, which are summarized in Table IV, indicate the particular importance of magnesium ions in organizing these two regions.

Methodological Problems. A few problems occurred in interpreting the data, some of which were outlined in the preceding paper (Douthwaite & Garrett, 1981). In general, there was no difficulty in aligning bands with either chemically modified control samples or water hydrolysis ladders. For the cobra venom and S_1 ribonucleases, 5′-end labeled samples moved behind the control band, as expected, but for the the 3′-end labeled RNA, whereas the cobra venom samples moved ahead of the control band, the S_1 ribonuclease sample moved anomalously behind the control band, presumably as a result of the reported 3′-phosphatase contamination of the latter. Band doubling was only observed at high enzyme concentrations due to the loss of the 3′-terminal Cp.

Radiolytic damage was again predominantly at U–A and C–A bonds; particularly prone were the bonds after U_{12}, C_{19}, C_{44}, Ψ_{50}, U_{54}, U_{62}, U_{78}, and C_{107}, and considerable care was necessary with ribonuclease A and T_2 results to avoid mistakes in identifying both primary cutting and secondary cutting. The problem was circumvented to a great extent by working quickly with low levels of radioactivity.

Discussion

The five-helix model in Figure 5 is based on phylogenetic studies of eukaryotic 5S RNAs (Garrett et al., 1981; Hori et al., 1980; Luehrsen & Fox, 1981). The extension of helix II into loop A to include base pairs U_{14}–A_{66} and C_{15}–G_{65} is also

based on phylogenetic results and has been considered in detail elsewhere (Peattie et al., 1981). The putative base pairs A_{27}–U_{53} and C_{28}–G_{52} in loop B, which are almost universal in eukaryotes and prokaryotes [e.g., Stahl et al. (1981)], are indicated with striated lines. All of the present data are considered with respect to this model.

Accessible Unpaired Nucleotides. These are indicated in Figure 5 by arrows that are approximately proportional to the degree of cutting. When a primary cut with one enzyme coincides with a secondary cut of another, as, for example, occurs at G_{37} (primary with ribonuclease T_1 and secondary with ribonucleases S_1 and T_2), it is considered a primary cut. Our findings of three very accessible regions at C_{10}–U_{12}, G_{37}–C_{39}, and U_{90}–G_{91} confirms and extends earlier studies. For example, Vigne et al. (1973) and Vigne & Jordan (1977) used ribonucleases A, T_1, and T_2 to demonstrate accessible regions at G_{37}–G_{41} and G_{91} in yeast 5S RNA and in all the other eubacterial and eukaryotic RNAs they tested. There have been conflicting reports, however, especially with ribonuclease S_1. For example, Nichols & Welder (1979) found no cuts at the above positions at pH 4.5, although they did with ribonuclease T_1 at pH 7.5. They found regions 12–25, 50–60, and 116–121 accessible at the optimum pH for the ribonuclease S_1 digestion (and in the absence of magnesium). Another study with ribonuclease S_1 on *Torulopsis utilis*, a fungus of sequence similar to *S. cerevisiae*, revealed cuts after nucleotides 12, 40, 57, and 110, apparently confirming the accessibility around position 37 but not G_{89}–A_{92} in loop D (Nishikawa & Takemura, 1977). Our data differ substantially from the latter two, in that we identified the major ribonuclease S_1 primary cuts at A_{11}, U_{12}, U_{38}, and C_{39} with weaker ones at U_{90} and G_{91}.

Recent studies on 5S RNA from rat liver (Toots et al., 1981) and from the silk moth *Bombyx mori* and slime mould *Dictyostelium discoideum* (Troutt et al., 1982) all reveal multiple cuts and exhibit major differences from one another and from the present study. For example, no cuts were observed in the rat liver RNA sequence C_{10}–U_{12} or in loop D, whereas they were found at U_{33}–G_{41} in loop C and at A_{74}–C_{78} and A_{101}–A_{103} in loop E. We classify some cuts in loop C as secondary and did not detect the cuts in loop E. The results for *B. mori* and *D. discoideum* show more general agreement with ours but substantial differences in detail; for example, no cuts were observed in the bulged region in helix IV (see below). We attribute most of the differences between the published data and ours on ribonuclease S_1 to our taking special care both to maintain the native conformation during the low pH digestion and to select for it again prior to analyzing for ribonuclease cuts.

Double-Helical Regions. The cobra venom ribonuclease has proved a useful probe of double helices and possibly of highly stacked single-stranded regions. The observed cuts provide strong support for helices I, II, and IV while the evidence for helices III and V, as indicated in Figure 4 and Table III, is less direct. The results also constitute strong evidence against the alternative cloverleaf model of Luoma & Marshall (1978) since the cuts from A_{17}–G_{21} fall in a single-stranded region of their model.

The studies on rat liver (Toots et al., 1981) and *B. mori* and *D. discoideum* 5S RNAs (Troutt et al., 1982) both employed the cobra venom ribonuclease. Again many differences are evident. For example, whereas extensive cutting was observed in helix III of rat liver and *B. mori* RNAs, none was observed in the *D. discoideum*. Cuts were also observed in loops B, C, and E of the *B. mori* RNA but not in the other RNAs. The main difference from our results is their greater number of cuts, which we attribute to their not selecting for the native conformer after digestion; thus they were also probing partially unfolded molecules (cf. Table III) and fragmented RNA.

Flexibility in the RNA Structure: Significance of Secondary Cutting. In general, the secondary cuts are adjacent to primary ones, and the local opening, as a consequence of the latter, seems readily comprehensible. For example, the ribonuclease S_1 cut at A_{51} follows the primary cut at Ψ_{50}.

There were some anomalies, however, as indeed there were in the eubacterial 5S RNA study, where one ribonuclease produced a primary cut at a given nucleotide and another generated a secondary cut. For example, ribonuclease T_1 is the only enzyme that induced primary cuts at G_{37} and G_{85}, whereas secondary cuts were produced at one or both nucleotides with ribonucleases S_1 and T_2. These exceptions, which probably only occur in the less accessible RNA regions, may reflect, first, the different properties of the ribonucleases, ribonuclease S_1 (M_r 65 000), for example, is much larger than the other enzymes, and, second, the differing modes of ribonuclease interaction with the RNA structure.

A major structural distortion was induced by the primary cuts at U_{38},C_{39} with ribonucleases S_1 and T_2, which resulted in secondary cutting for 15 to 20 nucleotides toward both 5′ and 3′ ends. The effect reflects some tension in this part of the molecule, even in the presence of 20 mM magnesium. Fox & Woese (1975) proposed that the relative instability of the eubacterial helix II might be exploited, in the ribosome, to produce a "tuning" effect on this RNA region (approximately nucleotides 25–55) that they assumed to be functionally important. It is possible that our data reflect such an effect although helix II is more stable in eukaryotes.

The flexibility in this large RNA region also correlates with two earlier studies. Vigne et al. (1973) showed that when yeast 5S RNA was cut at G_{37} and electrophoresed in polyacrylamide gels containing 40 mM Tris–acetate, pH 8.3, the two parts of the molecule (1–37 and 38–121) separated in spite of the extensive base pairing. In addition, Nishikawa & Takemura (1977) failed to obtain homogeneous ribonuclease S_1 digestion products of *T. utilis* RNA from the nucleotide sequences 14–32 at 20 °C and 12–57 at 37 °C; presumably part of these regions opened up to yield a series of heterogeneous fragments that were not detectable by their methods.

Nucleotides Bulged from Helices II and IV. Earlier, a nucleotide bulged from helix II was characterized in *E. coli* 5S RNA and shown to be common to all pro- and eukaryotic 5S RNAs; it is highly conserved as an adenosine in prokaryotes and yeasts, a cytidine in animals, and a uridine in plants. Evidence was provided that this accessible nucleotide is involved in ribosomal protein recognition (Peattie et al., 1981).

The present data are compatible with the looped out nature of this nucleotide in the *S. cerevisiae* 5S RNA. The cobra venom ribonuclease cuts occur adjacent to A_{64} in helix II, and cuts with ribonucleases S_1 and T_2 occur in this region as the magnesium is depleted. However, there are two possible base pairings of either A_{63} or A_{64} with U_{16} (see Figure 5). The former pairing best fits the phylogenetic comparisons and is favored by our data since stronger cutting occurs after A_{64} than after A_{63}, as magnesium is depleted (see Table IV).

Another potentially alternating bulge structure exists at A_{84}/G_{85} in helix IV that is exclusive to eukaryotes. It occurs within a protein binding region (Nazar, 1979) and has also been proposed as a protein recognition site (Garrett et al., 1981). Either A_{84} or G_{85} can be paired with U_{96}. Our data favor the latter pairing because of the ribonuclease A, S_1, and

T_2 cuts after U_{83}. However, the ribonuclease T_1 cut after G_{85} suggests that an equilibrium may exist, and this is further supported by the general flexibility observed in this region as magnesium is removed.

This bulged nucleotide is not so highly conserved as in helix II. Although it can be drawn as an adenosine for many 5S RNAs this often requires a shift of one base pair along helix IV; if the helix position is maintained, then the nucleotide can be A, U, or G. The structural flexibility observed in this region of the *S. cerevisiae* 5S RNA is almost universal in eukaryotes; either a G·U or U·U pairing is adjacent to the bulge or a potentially switching base pair is possible.

Highly Structured Regions and Tertiary Structure. The data yield a limited insight into the tertiary organization of the RNA. Some of the loop regions drawn in Figure 5 are very resistant to ribonuclease digestion. These include the sequences A_{22}–C_{28} in loop B, C_{34}–G_{36} and C_{40}–C_{44} in loop C, and A_{76}–A_{79} and G_{101}–C_{105} in loop E. Extensions to the secondary structure have been proposed which partially explain these resistances. For example, the pairing illustrated in Figure 5 between A_{27}–U and G_{52}–U is almost universal, although some structural flexibility would be required to explain the weak ribonuclease T_1 cut after G_{52}. A further pairing between U_{33}–C and G_{41}–A, proposed by Thompson et al. (1981) for *Drosophila* 5S RNA, is supported neither by the phylogenetic data (Luehrsen & Fox, 1981) nor by our ribonuclease digestion results.

We are left with the likelihood that these resistant regions, including helices III and V, are compactly folded in the tertiary structure. Vigne et al. (1973) have proposed base pairing between G_{37}-U-C and G_{91}-A-C that could facilitate such tertiary folding in eukaryotic 5S RNAs. However, only the U_{38}-C and G_{91}-A pairings are universally conserved in eukaryotes, and they are incompatible with our data, at least for the free 5S RNA.

Comparison with Other Data. (*a*) *Chemical Modification.* A few relevant studies have been made. 5S RNA of *T. utilis* was modified by using the guanosine-specific reagent kethoxal (Nishikawa & Takemura, 1978). The three most strongly modified guanosines G_{37} (0.5 mol), G_{57} (0.8 mol), and G_{91} (0.8 mol) that are conserved in the *S. cerevisiae* 5S RNA are indicated in Figure 5; two correspond to strong ribonuclease cutting positions, but the third, at G_{57}, is incompatible with our data. A further strong modification was observed in helix IV at G_{80}, G_{82}, and/or G_{85} (0.8 mol); our data suggest that G_{80} and G_{85} are the most likely sites.

Chemical cross-links were induced in *Drosophila* 5S RNA with psoralen (Thompson et al., 1981) and were localized between fragment pairs 22–30 and 49–56, and 76–82 and 84–97. The cross-linked nucleotides were tentatively assigned as U_{24}–U_{53} and U_{80}–U_{95} (or U_{96}); these assignments suggest additional base pairing in loop B and support the pairing in helix IV.

(*b*) *Physical–Chemical Studies.* Spectroscopic methods have been widely used to probe the secondary and tertiary structure of yeast 5S RNA. Estimates for the number of base pairs vary from an NMR study, giving 32 (±2) base pairs (Luoma et al., 1980), to an ultraviolet absorbance analysis indicating ≥40 base pairs (Luoma et al., 1980) and an infrared approach estimating 46 base pairs (Stulz et al., 1981) with a (G-C):(A-U) base-pair ratio of 1.1:1. Since the latter two methods detect non-Watson–Crick pairings involved in the tertiary structure, they may yield high estimates and, therefore, be incomparable with both the NMR estimate and the minimal secondary structural model presented in Figure 5.

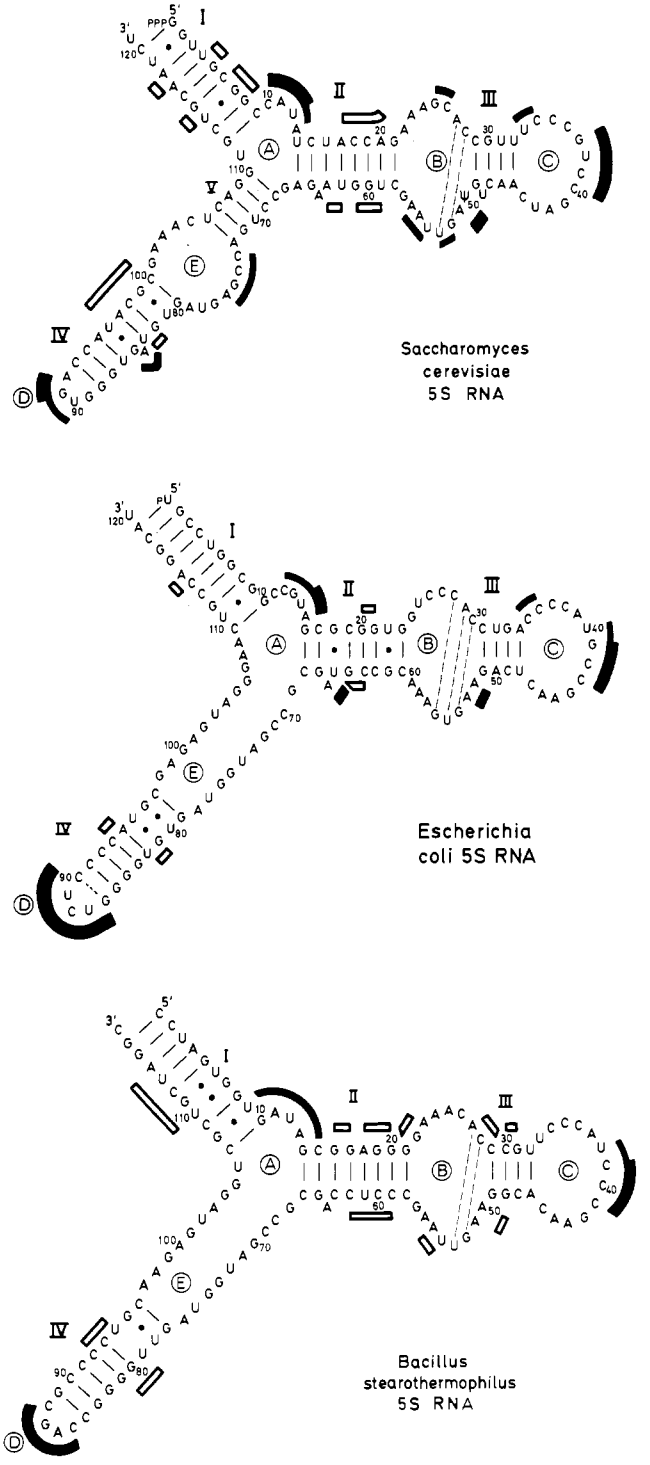

FIGURE 6: A comparison of ribonuclease digestion patterns of *S. cerevisiae*, *E. coli*, and *B. stearothermophilus* 5S RNAs. The results for the eubacteria are taken from Douthwaite & Garrett (1981) and are displayed on the modified Fox & Woese (1975) model. Filled and hollow lines correspond to single-strand- and double-strand-specific ribonuclease cuts, respectively. The thickness of the line is approximately proportional to the degree of single-strand cutting observed in that region; very weak cuts have been omitted.

However, the good correlation of the NMR data of Luoma et al. (1980) with the model in Figure 5 suggests that the latter contains most of the double-helical structure present in the RNA. The NMR estimate of a (G-C):(A-U) ratio of about 3:2 and no G-C or A-U-rich helical regions also correlates well. Lasar raman spectroscopy measurements are also compatible; they indicate that two-thirds of the uridines are base paired (70% in the model) with a high degree of stacking of guano-

sines and limited stacking of adenosines (Luoma & Marshall, 1978).

Comparison of Eubacterial and Eukaryotic RNAs. The ribonuclease digestion patterns for *S. cerevisiae*, *B. stearothermophilus*, and *E. coli* 5S RNAs are compared in Figure 6, and the results are summarized below. For helix I, more cuts are observed in the eukaryotic RNA, especially on the 5′ side of the helix. For helix II, similar digestion patterns occur, although fewer cuts in the *E. coli* helix may reflect its greater flexibility. The bulged nucleotide is accessible when adjacent to a G·U pair or when magnesium is depleted. Helix III is generally very resistant to all ribonucleases; only very weak cobra venom ribonuclease cuts occur in the *B. stearothermophilus* RNA. In helix IV, similar digestion patterns occur. The lower part of the helix is not cut. Single-strand-specific cuts are only induced at the bulged nucleotide in the eukaryote. For helix V, a regular double helix can only exist in the eukaryote; however, the region is invariably highly resistant to all ribonucleases.

Loop A contains a common very accessible sequence. Loop B is generally resistant. Only *S. cerevisiae* has a weak cut in the upper part of the loop (G_{25}). All RNAs exhibit a cut at the Ψ_{50}–A bond or at the corresponding A–A bond in eubacteria; for *B. stearothermophilus*, only, there is a weak cobra venom ribonuclease cut at the latter position, suggesting more stacking. Loop C contains both the most accessible RNA region and two highly resistant and conserved sequences C-C-C-Pu and C-G-A-A/U-C. The cut at the beginning of the loop was not detected in the *B. stearothermophilus* RNA. Loop D contains a common accessible region that is less strongly cut in the eukaryotic RNA. Loop E is highly resistant in the eubacteria whereas the eukaryote contains a sequence of limited accessibility.

In conclusion, the digestion patterns exhibit many common features. The yeast RNA tends to resemble the *E. coli* RNA more closely than that of *B. stearothermophilus*. The presence of more weak cobra venom ribonuclease cuts in the latter, especially in loop B and helix III, may indicate more efficient stacking to promote temperature resistance.

Acknowledgments

We appreciate the willing help of Anni Christensen and Steve Douthwaite and thank Professor Brian Clark for sharing the cobra venom ribonuclease.

References

Douthwaite, S., & Garrett, R. A. (1981) *Biochemistry 20*, 7301–7307.

Erdmann, V. A. (1976) *Prog. Nucleic Acid Res. Mol. Biol. 18*, 45–90.

Fox, G. E., & Woese, C. (1975) *Nature (London) 256*, 505–507.

Garrett, R. A., Douthwaite, S., & Noller, H. F. (1981) *Trends Biochem. Sci. (Pers. Ed.) 6*, 137–139.

Hori, H., Osawa, S., & Iwabuchi, M. (1980) *Nucleic Acids Res. 8*, 5535–5540.

Luehrsen, K. R., & Fox, G. E. (1981) *Proc. Natl. Acad. Sci. U.S.A. 78*, 2150–2154.

Luoma, G. A., & Marshall, A. G. (1978) *J. Mol. Biol. 125*, 95–105.

Luoma, G. A., Burns, P. O., Bruce, R. B., & Marshall, A. G. (1980) *Biochemistry 19*, 5456–5462.

Monier, R., & Feunteun, J. (1971) *Methods Enzymol. 20*, 494–502.

Nazar, R. N. (1979) *J. Biol. Chem. 254*, 7724–7729.

Nichols, J. L., & Welder, L. (1979) *Biochim. Biophys. Acta 561*, 445–451.

Nishikawa, K., & Takemura, S. (1974) *FEBS Lett. 40*, 106–109.

Nishikawa, K., & Takemura, S. (1977) *J. Biochem. (Tokyo) 81*, 995–1003.

Nishikawa, K., & Takemura, S. (1978) *J. Biochem. (Tokyo) 84*, 259–266.

Noller, H. F., & Woese, C. (1981) *Science (Washington, D.C.) 212*, 403–411.

Pace, B., Matthews, E. A., Johnson, K. D., Cantor, C. R., & Pace, N. R. (1982) *Proc. Natl. Acad. Sci. U.S.A. 79*, 36–40.

Peattie, D. A. (1979) *Proc. Natl. Acad. Sci. U.S.A. 76*, 1760–1764.

Peattie, D. A., Douthwaite, S., Garrett, R. A., & Noller, H. F. (1981) *Proc. Natl. Acad. Sci. U.S.A. 78*, 7331–7335.

Stahl, D. A., Luehrsen, R., Woese, C. R., & Pace, N. R. (1981) *Nucleic Acids Res. 9*, 6129–6137.

Stulz, J., Ackermann, Th., Appel, B., & Erdmann, V. A. (1981) *Nucleic Acids Res. 9*, 3851–3961.

Thompson, J. F., Wegnez, M. R., & Hearst, J. E. (1981) *J. Mol. Biol. 147*, 417–436.

Toots, I., Metspalu, A., Willems, R., & Saarma, M. (1981) *Nucleic Acids Res. 9*, 5331–5343.

Troutt, A., Savin, T. J., Curtiss, W. C., Celentano, J., & Vournakis, J. N. (1982) *Nucleic Acids Res. 10*, 653–664.

Vassilenko, S., & Babkina, V. (1965) *Biokhimiya 30*, 705–712.

Vigne, R., & Jordan, B. R. (1977) *J. Mol. Evol. 10*, 77–86.

Vigne, R., Jordan, B. R., & Monier, R. (1973) *J. Mol. Biol. 76*, 303–311.